Journal of Nuclear Materials 378 (2008) 349–357

Contents lists available at ScienceDirect

Journal of Nuclear Materials

journal homepage: www.elsevier.com/locate/jnucmat

Review

Thermodynamic study of actinides and lanthanides during total vaporisation of a very high burn-up UO_2 fuel

J.-P. Hiernaut *, P. Gotcu, J.-Y. Colle, R.J.M. Konings

European Commission, Joint Research Centre, Institute for Transuranium Elements, P.O. Box 2340, 76125 Karlsruhe, Germany

ARTICLE INFO

Article history:
Received 1 April 2008
Accepted 4 June 2008

ABSTRACT

A commercial PWR fuel sample of local burn-up of about 200 GWd/t was annealed in a Knudsen Cell Mass Spectrometer system (KCMS) with a temperature rate of 10 K/min up to 2750 K at which temperature the sample was completely vaporised. At high temperature the vapour above the sample contains mainly actinide and lanthanide oxides, the vapour pressure of refractory metals remaining below the detection limit. The local isotopic composition was determined by mass spectrometry and indicated a high content in higher actinides. From comparison of the partial vapour pressure with data for the pure oxides, obtained from experiments or literature, it is demonstrated that the actinide and lanthanide oxides dissolved in UO_2 matrix obey Henry's law.

Contents

1. Introduction

In a previous paper [1] we reported the release of fission gasses and volatile fission products from the pellet rim zone of a high burn-up fuel and correlated the results with the structural changes occurring at macro and micro scale during the annealing of the sample up to 2200 K. We observed that the matrix first re-crystallized from the typical high burn-up structure of the pellet rim to a structure close to the original one, and that most of the fission products were released. Above 2000 K vaporisation of the uranium oxide matrix became significant and at about 2700 K complete vaporisation occurred, including the fission and transmutation products dissolved in the matrix.

Since the concentration of the transuranium actinides and the lanthanides in this sample is relatively high as a result of the extremely high local burn-up, vaporisation studies in the temperature range between 1800 and 2700 K will give interesting and useful information about their activity coefficient in the uranium dioxide. In this paper we will present the partial vapour pressures of the transuranium actinides and the lanthanides in this sample and the stoichiometry evolution of the UO_2 matrix during the annealing process. The activities of the different compounds have been determined by comparison of the measured pressure data with

* Corresponding author. Tel.: +49 7247 951 385; fax: +49 7247 951 99 385.
E-mail address: Jean-Pol.Hiernaut@ec.europa.eu (J.-P. Hiernaut).

0022-3115/$ - see front matter © 2008 Published by Elsevier B.V.
doi:10.1016/j.jnucmat.2008.06.012

assessed values [2]or with new measurements on pure substances [3–8].

2. Experimental

The sample consisted of small pieces of 6 mg from the periphery ($1 > r/r_o > 0.91$) of a fuel pellet of cumulative average burn-up of 98 GWd/t, the mean local burn-up being 200 ± 20 GWd/t. The fuel characteristics and the irradiation history have been described in previous papers [9,10].

The sample was annealed and totally vaporised in a tungsten Knudsen cell coupled with a quadrupole mass spectrometer (KCMS). The Knudsen cell was heated in a high temperature furnace under high vacuum. The temperature of the cell was measured by a pyrometer in a black body hole bored in the cell itself. The technique and the system have been described in earlier publications [11–13]. The ionisation energy (E) was kept constant at 40 eV. This energy is sufficient to ionise all species but dissociation of molecular species occured also.

The KCMS system was calibrated by vaporising a known quantity of silver together with the sample. Silver is relatively inert in this system and vaporised completely at 1500 K, before the matrix evaporation started. From the ion intensities (I_{Ag}) of the silver isotopes ^{107}Ag and ^{109}Ag and the vapour pressure of silver (p_{Ag}) from Hultgren et al. [14] a global calibration factor of silver (K_{Ag}) was determined experimentally by using Eq. (1)

$$p_{Ag} = I_{Ag} \cdot T_{Ag} \cdot K_{Ag}. \quad (1)$$

The second-law vaporisation enthalpy of Ag found in our case is $\Delta_{vap}H = -(271.9 \pm 4.9)$ kJ/mol, which is in excellent agreement with the value derived from the recommendation of Hultgren et al. [14], $\Delta_{vap}H = -(269.5 \pm 2.0)$ kJ/mol, for the same temperature range.

Taking into account the ionisation cross section (σ) [15,16] and the appearance potentials (AP) of Ag and the species i measured, it is possible to determine the vapour pressure of any vaporising species i from their signals (I_i), as shown in Eq. (2)

$$p_i = I_i \cdot T_i \cdot K_{Ag} \cdot M_i^{1/2} \cdot B_i, \quad (2)$$

where

$$B_i = \frac{\sigma_{Ag}(E_{Ag} - AP_{Ag})}{M_{Ag}^{1/2} \cdot \sigma_i \cdot (E_i - AP_i)} \quad (3)$$

and M_i is the molar mass of species i. Under Knudsen-effusion conditions, the vapour pressure of species i at temperature T, is proportional to the mass effused (G_i), during the time Δt (scanning time interval of the measurement), i.e. Eq. (4) [17,18]

$$p_i = [G_i/(C \cdot S_{or} \cdot \Delta t)](2 \cdot \pi \cdot R \cdot T/M_i)^{1/2}, \quad (4)$$

where C is the Clausing factor (which is normally included in K_i), S_{or} the surface of the Knudsen cell orifice, and M_i the mass of species i. The quantity of every species effusing from the cell orifice per unit of time (G_i) is given by Eq. (5). The total quantity is obtained by summation of $G_i(\Delta t)$ over the total number of intervals (N)

$$\sum G_i = [1/(2 \cdot \pi \cdot R)^{1/2}] \cdot \sum (I_i \cdot T^{1/2} \Delta t \cdot K \cdot M_i \cdot B_i \cdot S_{or}), \quad (5)$$

where Δt is the length of a cycle (measured in seconds) and K the calibration factor.

The calibration factor was calculated from the integration of G corresponding to both isotopes ^{107}Ag and ^{109}Ag. With the calibration factor of silver (K_{Ag}) it is possible to calculate the quantity of each species i effusing through the Knudsen cell orifice at each temperature and during each time interval, and their corresponding partial vapour pressures. Applying this technique, the calculated $\sum G_{is}$ ('is' representing all the elements present in the sample and measured by mass spectrometry) is equal to the weight of the sample placed in the Knudsen cell with an uncertainty of 20%.

3. Evaluation of the results

The determined isotopic composition of the sample can normally be compared with the inventory of the sample calculated by Origen-2©. However, for the present sample this analysis was not possible because this code is not validated for calculations for the high burn-up of this sample (200 GWd/t).

To obtain the activity of actinide and lanthanide oxides in the uranium dioxide matrix, measured vapour pressures have been compared to values for the pure oxide compounds. If the actinides and lanthanides are perfectly soluble in the UO_2 matrix [3], resulting partial pressures obey Henry's law (6), i.e., they are directly proportional to the concentration of the corresponding compound in the solid phase, and the activity is equal to the concentration

$$p_i = x_i p^0 \quad (6)$$

or

$$x_i = p_i/p^0 \quad (7)$$

where p_i is the partial pressure of the species i, component in the total vapour amount, p^0 is the vapour pressure of the species i calculated for ideal conditions, and x_i is the mole fraction of the species i. Using Eq. (7), x_i can thus be obtained by comparison of the ordinates of the $\ln(p) = A + B/T$ curves of the high burn-up sample and the pure components. In case of ideal solution behaviour, x_i should be equal to the inventory of the initial sample derived from integration of G_i signals.

For actinide oxides of neptunium, americium, plutonium and curium the measurements were compared with the experimental results performed above the respective pure oxide compound in the same facility [11–13]. In parallel, the analysis was completed with a thermodynamic representation based on thermodynamic calculations for the actinides as well as the lanthanides. A thermodynamic database for the relevant solid and gaseous phases was compiled using data evaluated from different sources considered as the most accurate and recent [2,19–21]. Calculations were performed with the FactSage 5.5© software [22], a free energy minimisation program, for equilibrium composition and phases in conditions in a closed system (constant volume) at atmospheric pressure. For all the elements, the standard state data was taken from the FACT 53 compound database. Table 1 is dedicated comparisons of the equations of different linear fits for the vapour pressure measurements of this work and measured data above pure oxides.

For example, for La_2O_3 the different species present in the gaseous phase initially considered were La, La_2O, LaO, La_2O_2, LaO_2. FactSage 5.5© calculations for the vaporisation of this compound indicate that the partial pressures of LaO(g) and LaO_2(g) are about equivalent. However, experiments have shown that for vaporisation of La_2O_3 the predominant species in the gas phase is lanthanum monoxide [23]. The data available for LaO_2(g), which were estimated with large uncertainty ranges from ratios between some known atomisation energy values of the LnO_2(g) and LnO(g) molecules in the rare earth series [19,24], evidently overestimate the stability of LaO_2 [25]. For that reason data for the gaseous lanthanide dioxide species have been omitted, with the exception of CeO_2. The data for CeO_2 compound were obtained by direct measurements of cerium–oxygen system [26]. For similar reasons we have excluded PuO_3(g), though the existence of this molecule was claimed [27], being formed due to a chemical process involving oxygen adsorbed during oxidation of the sample.

Table 1
Equations of the different linear fits of the vapour pressure measurements (present experiment), and of measurements above pure oxides are given in K

Element	Measured data (present sample)	Measured data above pure oxides
Pu	$-(6.48 \times 10^4 \pm 0.3 \times 10^3) \times T^{-1} + (23.5 \pm 1.1)$	$-6.13 \times 10^4 \times T^{-1} + 28.0$[a] $-6.72 \times 10^4 \times T^{-1} + 30.0$ [28]
Am	$-(5.20 \times 10^4 \pm 0.3 \times 10^3) \times T^{-1} + (17.0 \pm 1.2)$	$-(5.91 \times 10^4 \pm 0.1 \times 10^3) \times T^{-1} + (25.4 \pm 0.1)$[a]
Np	$-(4.45 \times 10^4 \pm 0.3 \times 10^3) \times T^{-1} + (14.1 \pm 1.4)$	$-(6.48 \times 10^4 \pm 0.1 \times 10^3) \times T^{-1} + (29 \pm 0.1)$[a]
Cm	$-(7.86 \times 10^4 \pm 0.2 \times 10^3) \times T^{-1} + (26.8 \pm 0.1)$	$-(8.47 \times 10^4 \pm 0.1 \times 10^3) \times T^{-1} + (35.8 \pm 0.3)$
La	$-(7.58 \times 10^4 \pm 3.0 \times 10^3) \times T^{-1} + (27.8 \pm 1.2)$	$-(6.34 \times 10^4 \pm 0.1 \times 10^3) \times T^{-1} + (27.7 \pm 0.4)$
Ce	$-(4.85 \times 10^4 \pm 1.1 \times 10^3) \times T^{-1} + (16.8 \pm 0.5)$	–
Pr	$-(6.68 \times 10^4 \pm 1.4 \times 10^3) \times T^{-1} + (24.0 \pm 0.6)$	–
Nd	$-(7.42 \times 10^4 \pm 2.2 \times 10^3) \times T^{-1} + (27.6 \pm 0.9)$	$-(5.80 \times 10^4 \pm 0.1 \times 10^3) \times T^{-1} + (25.0 \pm 0.1)$
Sm	$-(6.78 \times 10^4 \pm 3.6 \times 10^3) \times T^{-1} + (24.5 \pm 1.4)$	–
Eu	$-(4.45 \times 10^4 \pm 7.0 \times 10^3) \times T^{-1} + (14.05 \pm 2.9)$	–

[a] The data from experiments performed in our lab and not yet published.

Thermodynamic data for this compound are limited to estimations on standard entropy and heat capacity [2] from quantum chemical calculations.

4. Results

4.1. Isotopic composition of actinides

The isotopic composition of actinides was determined from the $\sum G_i$ (Eq. (5)) and is reported in Table 2. For this high burn-up sample (>200 GWd/t), this composition is very different from lower burn-up (<60 GWd/t) uranium fuels but relatively close to the isotopic composition measured on mixed oxide fuels. It is thus clear that a large fraction of the fission products originate from Pu, Am, Cm. This could explain the very high ratio Xe/Kr determined in a previous paper on the same sample [1].

The following actinide isotopes were observed by mass spectrometry during high-temperature annealing: ^{234}U, ^{235}U, ^{236}U, ^{237}Np, ^{238}U, ^{238}Pu (<0.1%), ^{239}Pu, ^{240}Pu, ^{241}Pu, ^{241}Am, ^{242}Pu, ^{243}Am, and ^{244}Cm. These isotopes were detected as element, monoxide and dioxide. The U isotopes were also detected as trioxides. The mass spectrometric signals of the elemental actinides are presented in Fig. 1, which shows that most of the actinides were detected above 2100 K. The inventory of the different isotopes of actinides calculated from the $\sum G_i$, (with *i*, including the actinide metal ions plus its monoxide, dioxide and, for U, trioxide), is given in Table 2.

Table 2
Inventory of the sample: the amount of each element measured by Knudsen-effusion technique (Eq. (5)), given in μg and their concentration in % in the first three columns; the last column gives the data for measurements over pure oxides and for the assessments

Isotope	*w* (μg)	% (from sample)	% (from literature)	
			Pure oxide	Assessment
Sample	6000	1	–	–
^{234}U	2.866	0.0478	–	–
^{235}U	2.485	0.0414	–	–
^{236}U	22.722	0.3787	–	–
^{237}Np	8.093	0.1349	0.10 ± 0.004	0.12 ± 0.01[a]
^{238}U	5142.826	85.7138	–	–
^{239}Pu	41.479	0.6913	(0.32–0.48) ± 0.1	(0.17–0.74) ± 0.02
^{240}Pu	31.494	0.5249	–	–
^{241}PuAm	13.207	0.2201	–	–
^{242}Pu	16.587	0.2765	–	–
^{243}Am	7.124	0.1187	0.25 ± 0.08	0.26 ± 0.08[a]
^{244}Cm	6.973	0.1162	0.12 ± 0.02	0.15 ± 0.01
^{139}La	33.66	0.561	0.60 ± 0.07	1.1 ± 0.3
^{140,142}Ce	69	1.15	–	0.7 ± 0.1
^{141}Pr	27.797	0.4633	–	1.1 ± 0.07
^{143,144,145,146}Nd	79.328	1.3221	1.45 ± 0.2	3.1 ± 0.4
^{147,148,150,152}Sm	27.924	0.4654	–	3.0 ± 0.4
^{153}Eu	2.051	0.0342	–	–
^{156}Gd	0.936	0.0156	–	–

For ^{239}Pu the % range given is obtained from [29] and from measurements above pure oxide in our lab, for assessment between 1.5 and 2 stoichiometry range, respectively.

[a] The values assessed in the high temperature region concerning the highest volatilisation.

4.2. The actinides

4.2.1. Uranium

The vapour pressure of uranium oxides and their sum are plotted in Fig. 2 versus the inverse of the absolute temperature together with the assessed total pressure of UO_2. The $p(UO_3^+)$ signal is close to the UO^+ signal, and is only 8 times smaller than the UO_2^+ signal, which is typical for a hyper-stoichiometric sample. At high temperatures the UO_3^+ signal reaches a plateau and decreases, indicating reduction of the sample. The fact that the signal of UO_3^+ is approximately 1000 times larger than above $UO_{2.00}$ [28] indicates that most of the UO_2^+ signal comes from electrodecomposition of UO_3 [11], which is characteristic for the hyper-stoichiometric composition.

The slope of the $\sum UO_x$ (with $0 \leqslant x \leqslant 3$), line versus $1/T$ is -50.9 ± 0.16 kK (-423 kJ/mol), which is close to the slope of pUO_3 above U_4O_9: -49.4 kK (-410 kJ/mol), and much smaller than the slope of p^{tot} above UO_2 [19,22]: -67.8 kK (-564 kJ/mol).

The oxygen potential of this sample, as measured in another work [9], is about $\Delta G_{O_2} = -290$ kJ/mol at 1023 K, which is close to the value for $UO_{2.05}$ also obtained from the oxygen bearing signals of uranium species measurements [28–31]. The results from the present measurement (Fig. 3) show that the O/M ratio is quite scattered between 1500 and 2000 K, due to the poor signal to noise ratio in this temperature range, but remains larger than 2 up to 2100 K. Above this temperature, the UO_3^+ signal reaches a maximum and then starts to decrease, indicating a reduction of the sample. All the species we analysed vaporise at a temperature higher than 2100 K.

4.2.2. Neptunium

The vapour pressure of Np oxides above the high burn-up sample is plotted in Fig. 4. The species Np, NpO and NpO_2 were observed. The results are compared with recent measurements on pure NpO_2 [7]. At $T < 2200$ K, the results are representative for NpO_2 slightly hyper-stoichiometric. Above 2200 K the sample seems to get progressively reduced, and this is most likely responsible for the too small vaporisation enthalpy. The slope of Np bearing species ($\sum^{237}NpO_x$, with $0 \leqslant x \leqslant 2$) is -44.5 kK (-370 kJ/mol), smaller than the results obtained for pure NpO_2: -64.8 kK (-540 kJ/mol), and than the one assessed, -71.2 kK (-592 kJ/mol). The ordinate difference gives as concentration, 0.10%, not

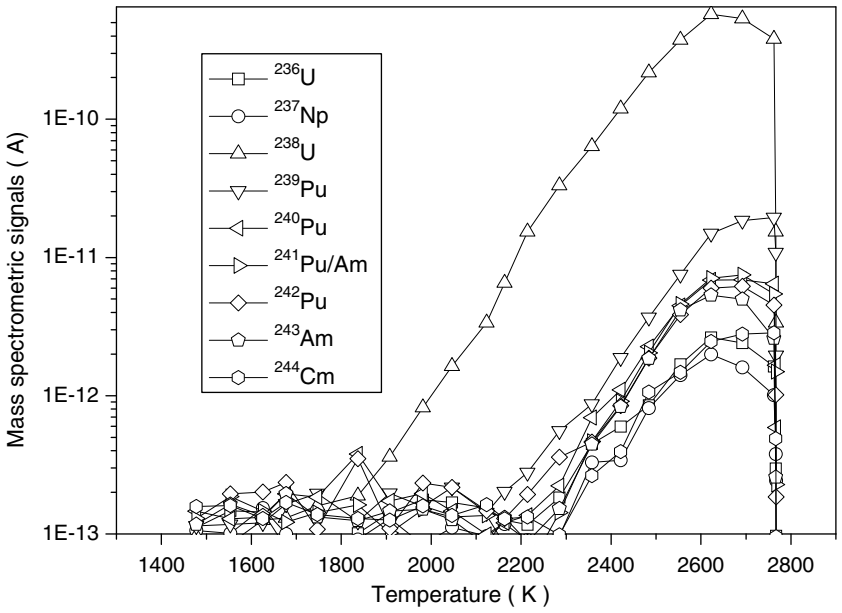

Fig. 1. The mass spectrometric signals of the elemental actinides plotted against the temperature range 1300–2800 K.

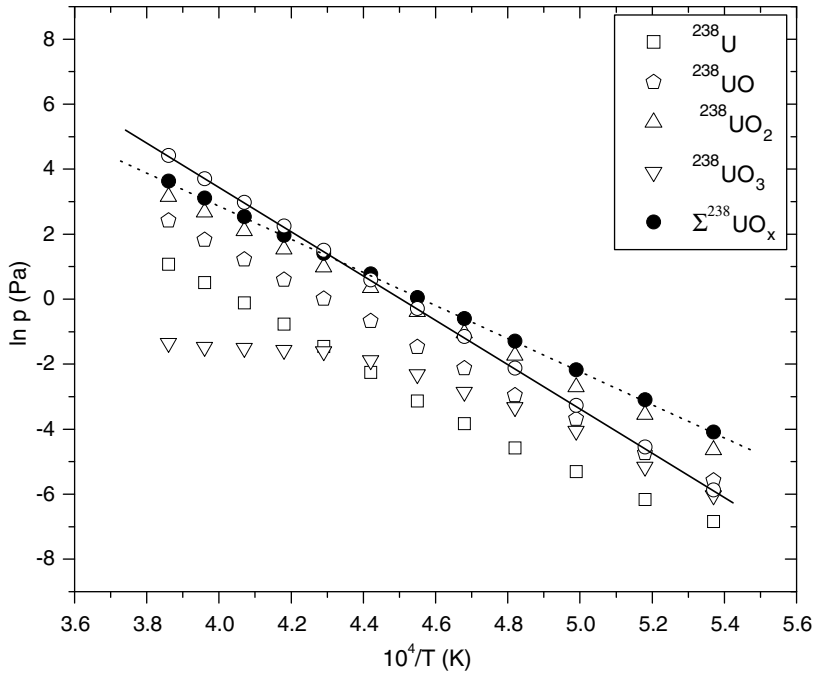

Fig. 2. The vapour pressure of the uranium oxides and their sum plotted versus the inverse of the absolute temperature. -○- assessed data; -●- pressure data measured above UO_2 in the present work. The index 'x' in $\sum UO_x$ varies between $x = 0$ and 3.

far from the value obtained by derivation of the thermodynamic calculation 0.12%, both values close to the value obtained by integration of G signal, 0.13% (Table 2), indicating that Henry's law is obeyed.

4.2.3. Plutonium

The assessed results reported here concern the main isotope ^{239}Pu, for which we derive a concentration of 0.69% for the inventory from integration of the G_i results (Table 2). The partial vapour pressures of the molecular Pu oxides and the total pressure of ^{239}Pu are plotted in Fig. 5. The measured vapour pressures show a discontinuity around 2350 K, the temperature at which the sample becomes hypo-stoichiometric. At lower temperature, the main species in the vapour is PuO_2, at higher temperatures, PuO and Pu, are the major contributors of the vapour. The slope of the vaporisation curve of Pu bearing species ($\sum^{239}PuO_x$, with $0 \leqslant x \leqslant 2$) between 2350 and 2700 K is −64.8 kK (−538 kJ/mol) which is close to the one calculated from measurements above pure oxide in our lab −61.3 kK (−510 kJ/mol).

This value can also be compared to that derived from the thermodynamic calculations. The observed vaporisation enthalpy agrees well between the range of the assessed vapour pressure

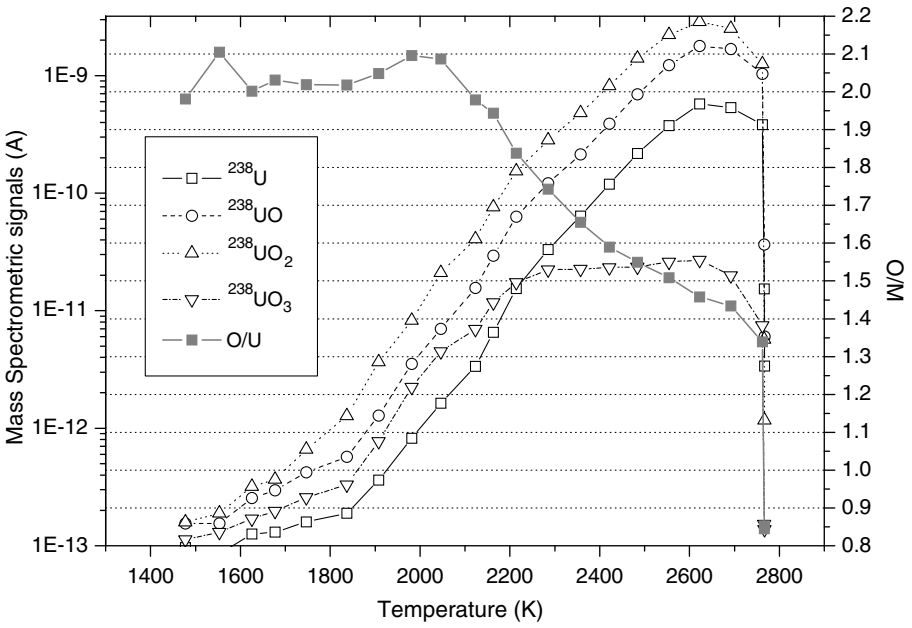

Fig. 3. The mass spectrometric signals (A) versus temperature (K). The secondary y-axis corresponds to the sample stoichiometry, O/U ratio, which varies along the temperature; at upper temperatures above 2000 K, the sample becomes hypo-stoichiometric.

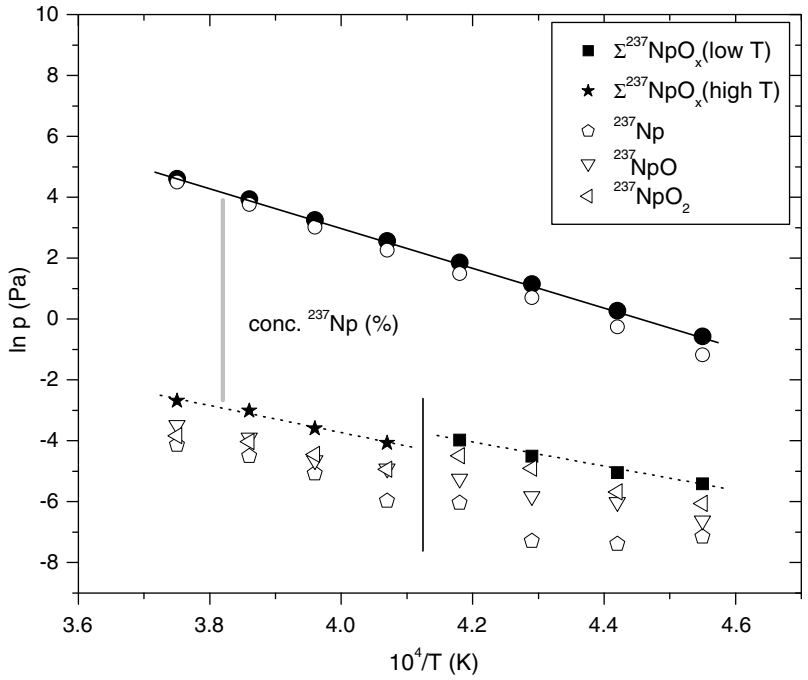

Fig. 4. The partial vapour pressure of the molecular Np oxides and the total pressure of ^{237}Np calculated from the sample. -●- pressure data measured above NpO_2 [7]; -○- assessed data. The index 'x' in $\sum^{237}NpO_x$ varies between $x = 0$ and 2.

above Pu_2O_3 and of that for PuO_2. This is in agreement with the fact that the congruent vaporisation composition of PuO_2 is at O/Pu < 2.0 [5]. Earlier literature data showed that solid PuO_2 vaporise congruently in the system [6] and the slope of the vaporisation curve is −67.2 kK (−558 kJ/mol) valid only in the temperature range 2000–2400 K and still very close to the one calculated from the experiments. Fig. 5 shows that the ordinate difference between the measured vapour pressure above the high burn-up sample and measured congruent vaporisation curve for PuO_2 varies between 0.32% and 0.48% above 2350 K and is close to 0.69% below this temperature, indicating that plutonium is soluble in the UO_2 matrix and follows Henry's law (6).

4.2.4. Americium

Americium has been analysed from the measurements of the ^{243}Am isotope, which are consistent with the results of mass 241, for which Am > Pu. The measured vapour pressure of Am and AmO for the high burn-up sample are plotted in Fig. 6. AmO_2 has not been included because its signal was too close to the detection limit. A small change of the ratio AmO/Am is observed around

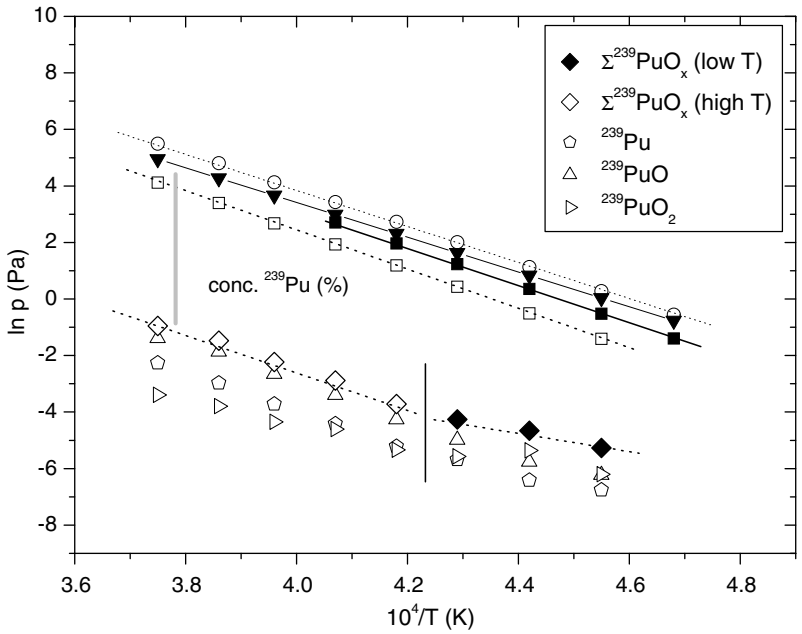

Fig. 5. The partial vapour pressure of the molecular Pu oxides and the total pressure of ^{239}Pu calculated from the sample. -○- pressure data from Pu_2O_3; -□- assessed data from PuO_2; -■- pressure data measured over congruently vaporising PuO_2 [6]; -▼- pressure data measured above pure PuO_2 (recently, in our lab). The index '*x*' in $\sum^{239}PuO_x$ varies between $x = 0$ and 2.

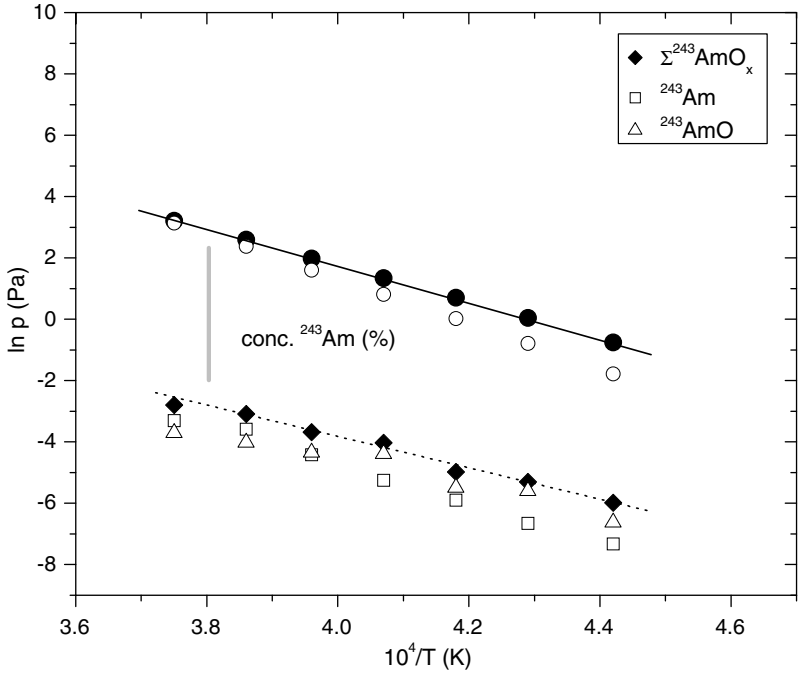

Fig. 6. The partial vapour pressure of the molecular Am oxides and the total pressure of ^{243}Am calculated from the sample. -●- pressure data measured above AmO_{2-x} [7]; -○- assessed data. The index '*x*' in $\sum^{243}AmO_x$ varies between $x = 0$ and 1.

2500 K. The total pressure is compared with the pressure measured above AmO_{2-x}, where *x* represents here a small uncertainty in the stoichiometry [7]. The slope obtained is −52.0 kK (−432 kJ/mol), again quite close to the slope obtained from measurements of AmO_{2-x}, −59.1 kK (−491 kJ/mol). The ordinate difference is 0.2–0.3% compared to 0.12% derived from integration of *G*. This discrepancy could be due to a small error in the determination of the pressure due to the lack of knowledge of σ (electron cross section) and the appearance potential of Am. The thermodynamic calculations for the vapour above Am_2O_3 indicate a different slope, −73.7 kK (−613 kJ/mol). However, the calculations also show a strong dependence on the oxygen potential. Realising that the uncertainties of the thermodynamic functions of the americium phases and species are relatively large [2,21], we can also claim that Henry's law is approximately respected for americium oxide dissolved in the UO_2 matrix.

4.2.5. Curium

Curium was the last actinide detected in the high burn-up sample. ^{244}Cm and ^{244}CmO were observed, but $^{244}CmO_2$ was not detected. The results are plotted in Fig. 7 and compared with the total pressure for Cm_2O_3 obtained from previous measurements [3], which is in good agreement with the calculated vapour pressure using thermodynamic data. The slope of total pressure of curium bearing species ($\sum^{244}CmO_x$, with $x = 0$ and 1) is slightly smaller than the slope determined in the experiment: −78.6 kK (−653 kJ/mol) compared to −84.7 kK (−704 kJ/mol). The difference between the two curves corresponds to $x_{Cm} = 0.12$, which is almost identical with the value obtained by integration of G signal, 0.116% (Table 2), indicating that Henry's law is obeyed.

4.3. The lanthanides

All the lanthanides from lanthanum to gadolinium have been detected in the vapour phase both as element and monoxide. Cerium has also been detected as dioxide at temperatures higher than 2000 K. The different isotopes observed are ^{139}La, ^{140,142}Ce,

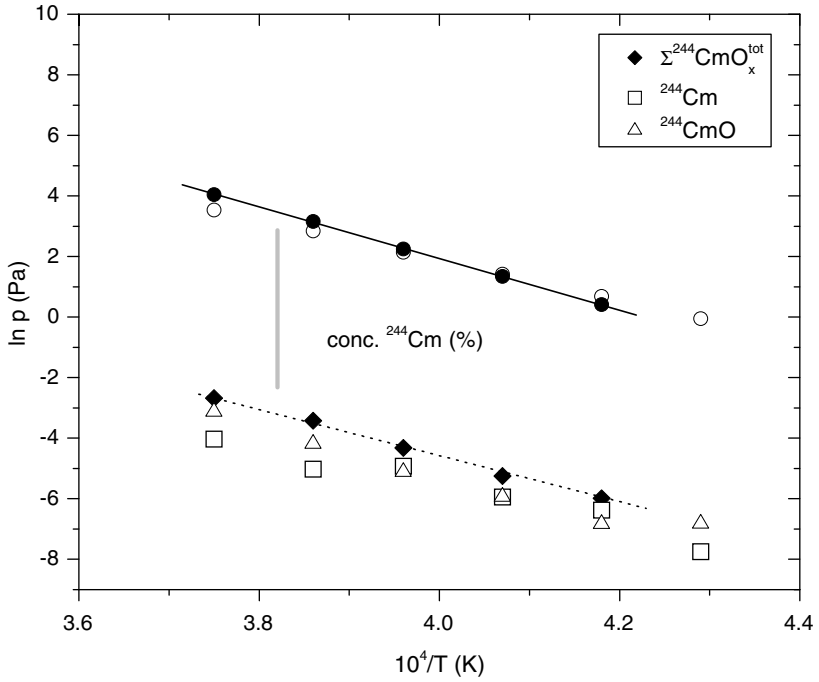

Fig. 7. The partial vapour pressure of the molecular Cm oxides and the total pressure of ^{244}Cm calculated from the sample. -●- pressure data measured above Cm_2O_3 [3]; -○- assessed data. The index 'x' in $\sum^{244}CmO_x$ varies between $x = 0$ and 1.

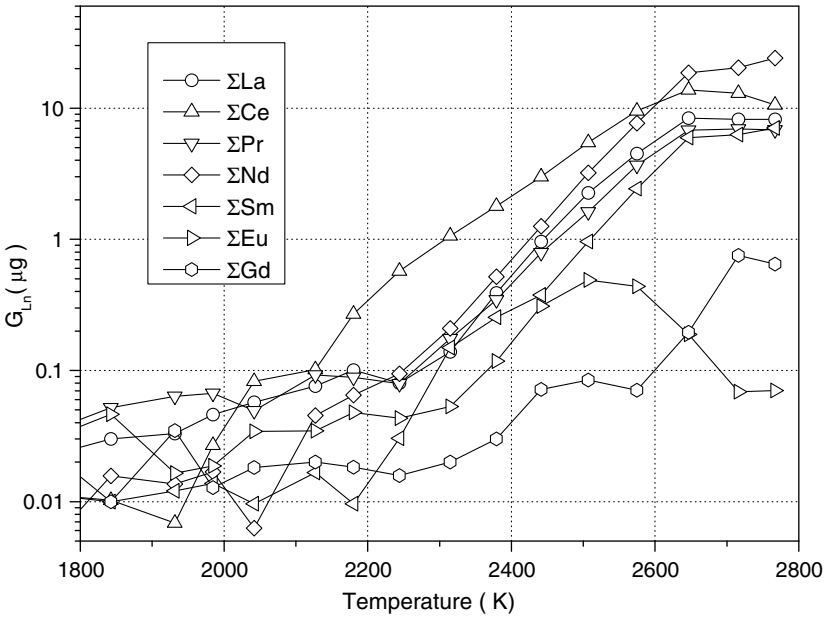

Fig. 8. The sum of the species leaving the Knudsen cell per time interval of a measuring cycle.

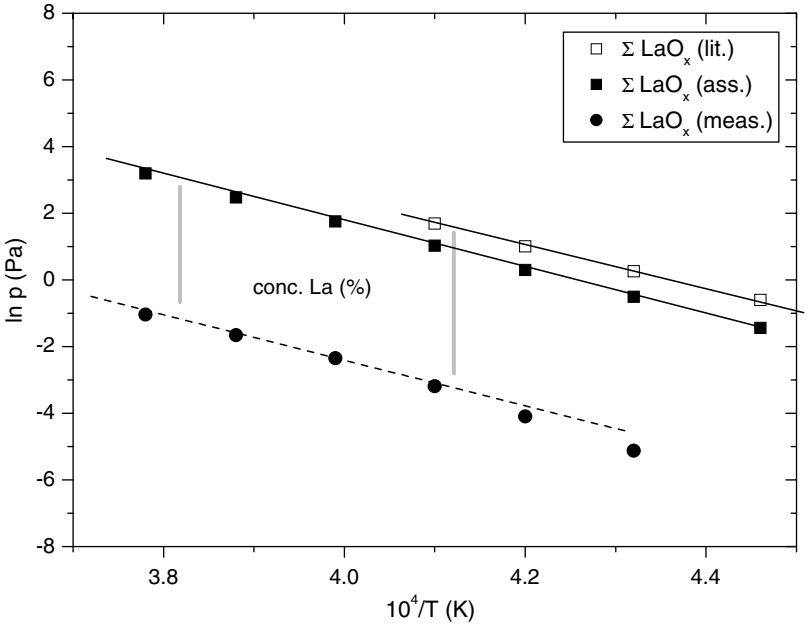

Fig. 9. The total pressure of La bearing species. -●- measured data over the high burn-up sample; -■- assessed data; -□- is the data from [8] for a maximum temperature of 2441 K. The index '*x*' in $\sum LaO_x$ varies between $x = 0$ and 1.

^{141}Pr, ^{143,144,145,146}Nd, ^{147,148,150,} ^{152}Sm, ^{153}Eu, and ^{156}Gd. Pm was not detectable. Interferences (such as CeO and CeO_2 with Gd and GdO, and Nd, ^{148}Sm and ^{150}Sm, respectively) were partly solved considering the isotopic composition of these elements. The interferences between ^{134,136,137,138}BaO and ^{150,152}Sm, ^{153}Eu, ^{154}(Eu, Sm, Nd) could be solved by the fact that BaO is released at lower temperature [1].

The sum of the $(M + MO + MO_2)$ species leaving the Knudsen cell per time interval of a measuring cycle is plotted in Fig. 8 for all the lanthanides. The most abundant elements are Nd and Ce, whereas Gd and Eu are just above the detection limit and the results are too imprecise to be taken into account. The total vapour pressures of the lanthanide oxides vaporising from the sample are compared to the assessed pressures above the pure lanthanide oxides showing that the concentrations of the La, Nd, Pr, Sm species are higher than the inventory from integration of *G* signals (Table 2). In contrast, Ce concentration was found to be lower than the inventory. For La and Nd, comparisons were made with literature data for the congruent vaporisation composition [8], yielding concentrations close to the inventory (Figs. 9 and 10). This reflects the strong change of the oxygen potential during the vaporisation of the sample. But on the basis of the last observation, it can be concluded that the lanthanides in irradiated fuel also obey, with a good approximation, Henry's law.

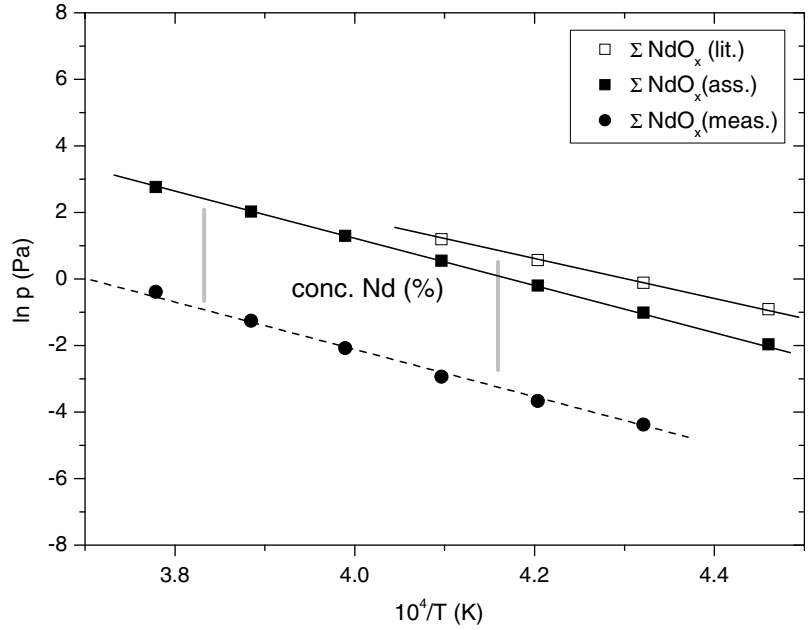

Fig. 10. The total pressure of Nd bearing species. -●- measured data over the high burn-up sample; -■- assessed data; -□- data from [8] for a maximum temperature of 2434 K. The index '*x*' in $\sum NdO_x$ varies between $x = 0$ and 1.

5. Conclusion

The vaporisation of the actinide and lanthanide oxides from a high burn-up UO_2 sample was studied. The actinide isotopic inventory was determined by mass spectrometry for this very high burn-up UO_2 sample on which no reliable Origen-2© calculation is possible. It shows a very high content in higher actinides. Comparison to the vaporisation of the pure oxide phases has shown that the transuranium actinide and lanthanide elements in the spent fuel follow, with a good approximation Henry's law, indicating near ideal solution behaviour.

References

[1] J.-P. Hiernaut, T. Wiss, J.-Y. Colle, H. Thiele, C.T. Walker, W. Goll, R.J.M. Konings, J. Nucl. Mater. 377 (2008) 313.
[2] L.V. Gorokkov et al., Institute for High Temperatures, Joint Institute for High Temperatures, Russian Academy of Sciences, Moscow, Russian Federation 2007.
[3] J.-P. Hiernaut, C. Ronchi, J. Nucl. Mater. 334 (2004) 133.
[4] S. Sunder, R. McEachern, J.C. LeBlanc, J. Nucl. Mater. 294 (2001) 59.
[5] H.A. Wriedt, Bull. Alloy Phase Diagrams 11 (1990) 184.
[6] R.N.R. Mulfort, L.E. Lamar, in: E. Grison, W.B.H. Lord, R.D. Fowler (Eds.), Plutonium 1960, London 1961, p. 411.
[7] P. Gotcu, JRC-ITU-TN-75, 2006.
[8] H.W. Goldstein, P.N. Walsh, D. White, J. Chem. Phys. 65 (1961) 1400.
[9] C.T. Walker, V.V. Rondinella, D. Papaioannou, S.V. Winckel, W. Goll, R. Manzel, J. Nucl. Mater. 345 (2005) 192.
[10] C.T. Walker, D. Staicu, M. Sheindlin, D. Papaioannou, W. Goll, F. Sontheimer, J. Nucl. Mater. 350 (2006) 19.
[11] F. Capone, J.Y. Colle, J.-P. Hiernaut, C. Ronchi, J. Phys. Chem. A 103 (1999) 10899.
[12] F. Capone, J.-P. Hiernaut, M. Martellenghi, C. Ronchi, Nucl. Sci. Eng. 124 (1996) 436.
[13] J.Y. Colle, J.-P. Hiernaut, D. Papaioannou, C. Ronchi, A. Sasahara, J. Nucl. Mater. 348 (2006) 229.
[14] R. Hultgren, R.L. Orr, P.D. Anderson, K.K. Kelley, Selected Values of Thermodynamic Properties of Metals and Alloys, John Wiley & Sons, Inc., 1963.
[15] J. Mann, J. Chem. Phys. 46 (1967) 1646.
[16] J.W. Otvos, D.P. Stevenson, J. Am. Chem. Soc. 8 (1956) 546.
[17] G. Chaudron, F. Trombe, Les hautes températures et leurs utilisations en physique et en chimie, Masson et Cie, Paris, 1975. p. 121.
[18] R. Grimley, in: J. Margrave (Ed.), The Characterisation of High Temperature Vapors, John Wiley, NY, 1967.
[19] V.P. Glushko, L.V. Gurvich, G.A. Bergman, I.V. Veyts, V.A. Medvedev, G.A. Khachkuruzov, V.S. Yungman Thermodynamic Properties of Individual Substances (Termodinamicheskie Svoistva Individual'nykh Veshchestv), Nauka, Moscow, 1982.
[20] R.J.M. Konings, L.R. Morss, J.Fuger, Chapter 19: The Chemistry of the Actinide and Transactinide Elements, Springer, Dordrecht, The Netherlands, 2006.
[21] R.J.M., Konings, D. Sedmidubsky, JRC-ITU-TN-20, 2005.
[22] FactSage 5.5© 2007, Developed at the Facility for the Analysis of Chemical Thermodynamics (FACT), Centre for Research in Computational Thermochemistry (CRCT), École Polytechnique de Montréal, Canada, and GTT Technologies, Herzogenrath, Germany.
[23] R.J. Ackermann, E.G. Rauh, J. Chem. Thermodyn. 3 (1971) 445.
[24] J. Kordis, K.A. Gingerich, J. Chem. Phys. 66 (1977) 483.
[25] M. Heyrman, C. Chatillon, A. Pisch, Comput. Coupling Phase Diagrams Thermochem. 28 (2004) 49.
[26] R.J. Ackermann, E.G. Rauh, J. Chem. Thermodyn. 3 (1971) 609.
[27] C. Ronchi, F. Capone, J.Y. Colle, J.-P. Hiernaut, J. Nucl. Mater. 280 (2000) 111.
[28] J.-P. Hiernaut, J.-Y. Colle, R. Pflieger-Cuvellier, J. Jonnet, J. Somers, C. Ronchi, J. Nucl. Mater. 344 (2005) 246.
[29] H. Matzke, J. Nucl. Mater. 208 (1994) 18.
[30] H. Matzke, J. Nucl. Mater. 223 (1995) 1.
[31] H. Matzke, J. Ottaviani, D. Pellottiero, J. Rouault, J. Nucl. Mater. 160 (1988) 142.